DOI: 10.1016/j.jcou.2017.02.007

NMR spectroscopic investigations into the mechanism of absorption and desorption of CO_2 by (tris-pyridyl)amine Zn complexes

Bjørnar Arstad,[1] Richard Blom,[1] Terje Didriksen,[1] Morten Frøseth,[1] Richard H. Heyn,*[1] and Sigurd Øien-Ødegaard[2]

[1] *SINTEF Materials and Chemistry, P. O. Box 124 Blindern, 0314 Oslo, Norway*

[2] *Department of Chemistry, University of Oslo, P. O. Box 1033 Blindern, 0371 Oslo, Norway*

rhh@sintef.no

Abstract

The Zn complex $[(NN3)Zn(OH)]_2(NO_3)_2$ (**1(NO$_3$)$_2$**, NN3= tris(2-pyridylmethyl)amine) reacts with atmospheric CO_2 to form a zinc carbonate species $\{[(NN3)Zn]_3CO_3\}(NO_3)_4$ (**2(NO$_3$)$_4$**), isolable as a crystalline product from organic solvents. The aqueous chemistry of the CO_2 absorption and desorption processes for **1(NO$_3$)$_2$** and the presumed end-point of the reaction, **2(NO$_3$)$_4$**, was unknown and hence investigated by NMR spectroscopy. Carboxylation of aqueous solutions of both **1(NO$_3$)$_2$** and **2(NO$_3$)$_4$** form products that can best be described as mixtures of monomeric $[(NN3)ZnCO_3H]^+$ and dimeric $\{[(NN3)Zn]_2CO_3\}^{2+}$, which are in a dynamic equilibrium on the NMR time-scale. No evidence for the involvement of **2(NO$_3$)$_4$** in the carboxylation-decarboxylation processes is observed. Rather, the data suggest that **2(NO$_3$)$_4$** provides $[(NN3)Zn(OH_2)]^{2+}$ that does not participate in the CO_2 chemistry upon warming. A mechanism that is supported by NMR experiments and that accounts for the formation of $[(NN3)ZnCO_3H]^+$ and $\{[(NN3)Zn]_2CO_3\}^{2+}$ from both ends of the reaction manifold is proposed.

DOI: 10.1016/j.jcou.2017.02.007

1. Introduction

First generation, large-scale capture of CO_2 from flue gas emitted from a power-generation facility or other industrial sources relies on aqueous solutions of monoethanolamine (MEA) or advanced amines.[1] The process involves the absorption of CO_2 to give bicarbonate and carbamate species at 40-50 °C. Regeneration by stripping of the CO_2 at 120-140 °C requires heating and cooling of large amounts of water, with corresponding energy penalties. For most amines, and in particular for MEA, the elevated temperature needed for regeneration causes decomposition, with corresponding material penalties for replenishment of amine and disposal of amine salts.[2] The process would become much more economically viable if alternative, more stable CO_2 capture reagents that required a smaller temperature swing could be developed. This would decrease the associated material and energy penalties and make such CO_2 capture processes more suitable for the large scales required for carbon dioxide capture and storage (CCS) schemes. A large number of water-soluble, nitrogen-containing absorbents, and blends of such, have been studied, and incremental improvements in the CO_2 capture penalty have been achieved.[3]

In the search for improved post-combustion capture technologies that can readily replace or augment the MEA process, or potentially catalyze CO_2 capture processes, a number of groups have looked at utilizing the enzyme carbonic anhydrase (CA), which catalyzes the hydration of CO_2. CA has been shown to promote CO_2 sorption in potassium carbonate solvents.[4] CA has also been immobilized on a porous carbon support and its activity and stability in a MDEA CO_2 capture solution has been investigated.[5] Since the natural enzymes have stability challenges under the conditions used in the MEA process,[6] artificial CA mimics have also been investigated. The CO_2 hydration and dehydration kinetics of $[LM]^{2+}$ (L = nitrilo-tris(2-benzimidazoylmethyl-6-sulfonic acid), M = Zn, Cd, Co; L = tris(2-benzimidazoylmethyl)amine, M = Zn) and $[M(cyclen)]^{2+}$ (M = Zn, Cu; cyclen = 1,4,7,10-tetraazacyclododecane) have recently been studied, and a pH swing process has been proposed on the basis of the results.[7] Computationally derived activation energies and experimentally determined CO_2-hydration rate constants have been compared for a series of Zn(II) aza-macrocycles.[8] The aforementioned $[Zn(cyclen)]^{2+}$ salt was evaluated under the industrial carbon capture process conditions of high pH, saturated K_2CO_3 concentrations, and elevated temperatures, and it showed significant catalytic activity even after several days at 130°C.[9]

DOI: 10.1016/j.jcou.2017.02.007

One relatively large class of compounds that have not been studied as potential post-combustion CO_2 capture materials is transition metal complexes known to absorb CO_2 directly from the atmosphere. These complexes are primarily based on Zn and Cu, and many of these compounds are hydroxides with a coordination sphere that loosely mimics that of the active site of CA,[6] while others are coordinated by macrocycles such as Schiff bases. The products of the reaction with atmospheric CO_2 are then primarily carbonates, although the carbonate moiety can take a number of different coordination modes, as shown in Scheme 1.[10] Complexes with μ_5- and μ_6-carbonates can also be formed.[11] The hypothesis was that such compounds might be interesting candidates for absorption of CO_2 from flue gas. Since these compounds react with atmospheric CO_2, the relatively low concentrations of CO_2 in flue gas (on the order of 4-15 %) should not represent a reactivity issue. It was further expected that these materials, as loose analogues to CA, should have high selectivity for CO_2 and be

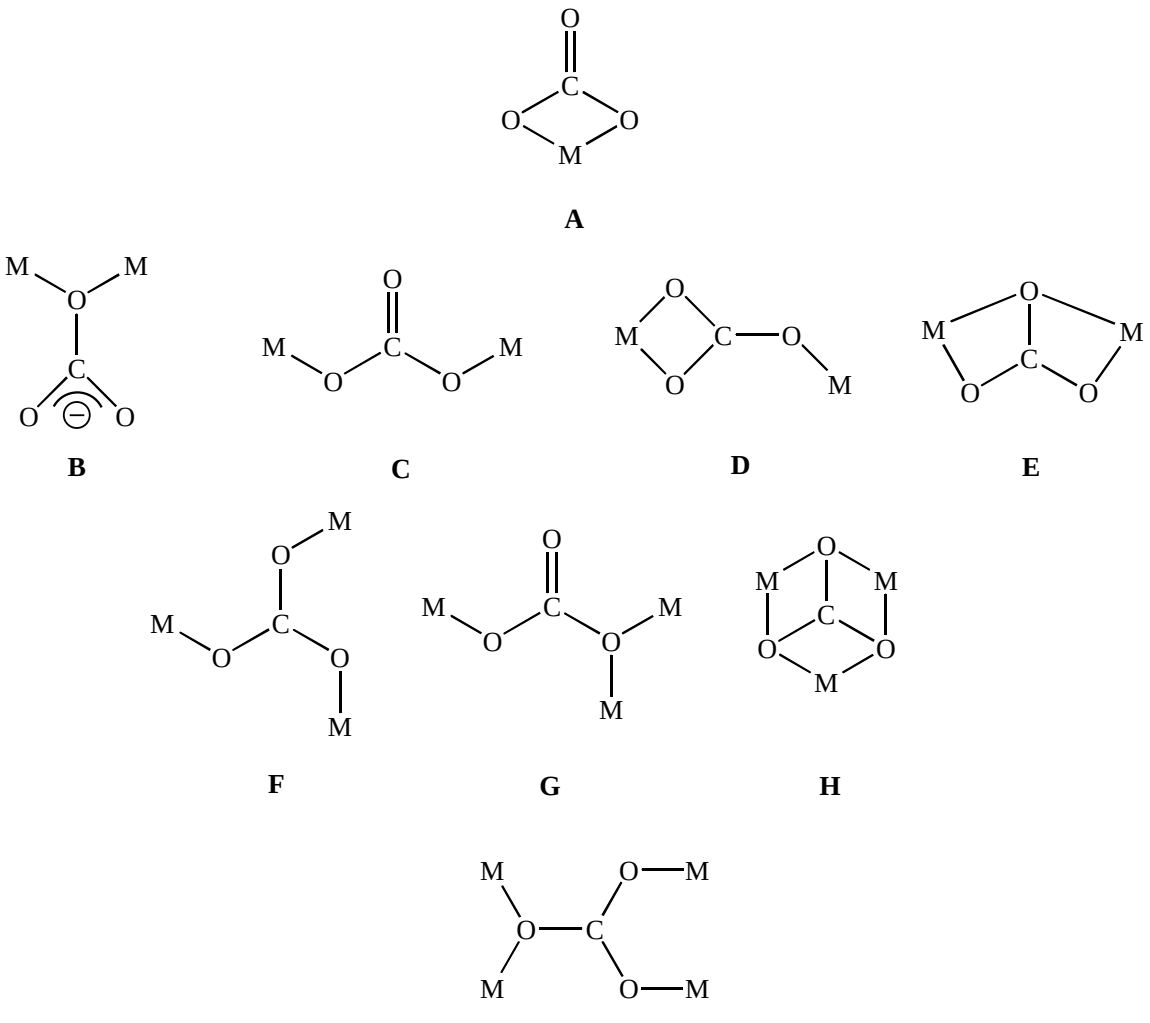

Scheme 1. Carbonate coordination modes in complexes derived from atmospheric CO_2.

DOI: 10.1016/j.jcou.2017.02.007

relatively less sensitive to the other components of flue gas, primarily water, and waste gasses such as SO_x and NO_x.[12]

A survey of the literature on this class of transition metal complexes showed that the absorption step has been of primary interest. The subsequent desorption step – or even the reversibility of the absorption-desorption process – have very rarely, if ever, been investigated. As well, NMR investigations *in water* of either CA mimics or transition metal complexes that absorb atmospheric CO_2 have, as far as we can tell, never been reported. Thus, there exist fundamental questions regarding the mechanism of the aqueous absorption and desorption processes, the reversibility of these process, and the involvement of the isolated metal-carbonate products. From the general considerations of the speed of the reaction with atmospheric CO_2, the compatibility of the system with water, and the amenity of the system towards study by NMR spectroscopy, the transition metal complex, $[(NN3)Zn(\mu_2\text{-}OH)_2Zn(NN3)](NO_3)_2$ (**1(NO$_3$)$_2$**, NN3 = tris(2-pyridylmethyl)amine),[13] and its crystalline carboxylation product $\{[(NN3)Zn]_3CO_3\}(NO_3)_4$ (**2(NO$_3$)$_4$**)[14] were chosen as the best candidates for a detailed mechanistic investigation. The more global properties of this system, such as the absorption capacities and kinetics of aqueous solutions of **1(NO$_3$)$_2$**, have recently been published elsewhere.[15]

2. Experimental

Unless otherwise indicated, reagents and solvents were obtained from commercial suppliers and used as received. NN3 was synthesized via a literature procedure[16] or purchased from Chemieliva Pharmaceutical Co. Ltd. (purity 98%) and recrystallized from diethyl ether before use. Methanol was degassed with argon prior to use. **1(NO$_3$)$_2$** and **2(NO$_3$)$_4$** were synthesized by slight modification of a published procedure,[13] substituting $Zn(NO_3)_2 \cdot 6H_2O$ for $Zn(ClO_4)_2 \cdot 6H_2O$. Their ^1H and ^{13}C NMR chemical shift data are contained in the Supporting Information.

Synthesis of 1(NO$_3$)$_2$. Under argon, a mixture of $Zn(NO_3)_2 \cdot 6H_2O$ (10g, 33.6mmol) and NN3 (9.76g, 33.6mmol) in 200 mL methanol was stirred vigorously and to that a 20 mL methanol solution of KOH (1.89 g, 33.6 mmol) was added. KNO_3 precipitated immediately, but the mixture was stirred at room temperature overnight. KNO_3 was removed by filtration through celite. Methanol was removed under vacuum providing 11.6 g (13.3 mmol, 81 % yield) of a white powder.

DOI: 10.1016/j.jcou.2017.02.007

Synthesis of $2(NO_3)_4$. A stream of CO_2 was blown into a solution of $\mathbf{1(NO_3)_2}$ (0.65 g, 0.75 mmol) in CH_3NO_2 (50 ml) for 7 min. There was no observable color change, apart from some hazing of the solution. After stirring for 30 min, the mixture were filtrated through celite and the volatiles removed to give $\mathbf{2(NO_3)_4}$ as a pale yellow solid (0.49 g, 0.37 mmol, 74 % yield). The solid was recrystallized from a CH_3NO_3 solution layered with diethyl ether, providing clear, needle-like crystals.

Sample preparation for NMR experiments. Samples were prepared by dissolving weighed amounts of material in fresh D_2O under an argon atmosphere. 99.9 % ^{13}C CO_2 enriched gas was bubbled through the solution in the NMR tube for 5 minutes.

NMR experiments. NMR experiments were performed at 9.4 T (proton resonance frequency of 400 MHz) with a Bruker Avance III spectrometer using a BBFO Plus double resonance probe head at 298.15 K; D_2O was used for locking purposes. The spectra were processed using MestreNova software, and all shift values were referenced to TMS via the substitution method.[17] 1D ^{1}H, ^{13}C and $^{13}C\{^{1}H\}$ spectra and 2D COSY, HSQC, and HMBC spectra were collected. ^{13}C EXchange SpectroscopY (EXSY) experiments were performed on a solution of $\mathbf{1(NO_3)_2}$ and CO_2 using a standard phase sensitive NOESY pulse sequence with a mixing time of 0.5 µs to observe qualitatively the chemical exchange pathways of the C-atoms. Temperature calibrations were done using methanol chemical shift variations. Integrated $^{13}C\{^{1}H\}$ spectra were obtained with a 30 s pulse delay using an inverse gated decoupling pulse sequence and 40 scans. Tests of various recycle delay lengths showed that these values were satisfactory for quantitative data with a good S/N ratio. Except for the experiment providing chemical exchange data, the concentration of Zn in all experiments was kept constant at 0.15 M, corresponding to 6.5 wt.% $\mathbf{1(NO_3)_2}$ and 7.2 wt % $\mathbf{2(NO_3)_4}$.

3. Results

3.1. Synthesis and characterization of $\mathbf{1(NO_3)_2}$ and $\mathbf{2(NO_3)_4}$

Since investigation of the global properties of these Zn complexes as CO_2 capture reagents required large scale synthesis on the order of several hundred grams, and due to the known explosive potential of perchlorate salts, particularly when handling large quantities of solid materials,[18] nitrate anions were substituted for the perchlorate anions used in the original synthesis.[13] Thus, $Zn(NO_3)_2 \cdot 6H_2O$ was treated with NN3 and KOH in degassed methanol under argon, due to the reported reactivity of $\mathbf{1(ClO_4)_2}$ towards atmospheric CO_2. The addition of KOH induced an immediate precipitation of KNO_3, and a white crystalline

DOI: 10.1016/j.jcou.2017.02.007

product was collected by evaporation of methanol. The ^{1}H NMR spectrum of **1(NO$_3$)$_2$** was identical to that reported for **1(ClO$_4$)$_2$**.[13]

The synthesis of **2(NO$_3$)$_4$** likewise followed the reported procedure, either by stirring a solution of **1(NO$_3$)$_2$** in air or by bubbling CO_2 through the solution, as shown in Scheme 2. Bubbling of CO_2 immediately caused a small amount of precipitate that was removed by filtration through celite. Evaporation of the solvent formed a yellowish-white product. The ^{1}H NMR spectrum of the product was identical to that reported for **2(ClO$_4$)$_4$**.[13] The product was recrystallized by carefully layering diethyl ether over a nitromethane solution of **2(NO$_3$)$_4$**, and after three days nice needle-shaped crystals could be collected.

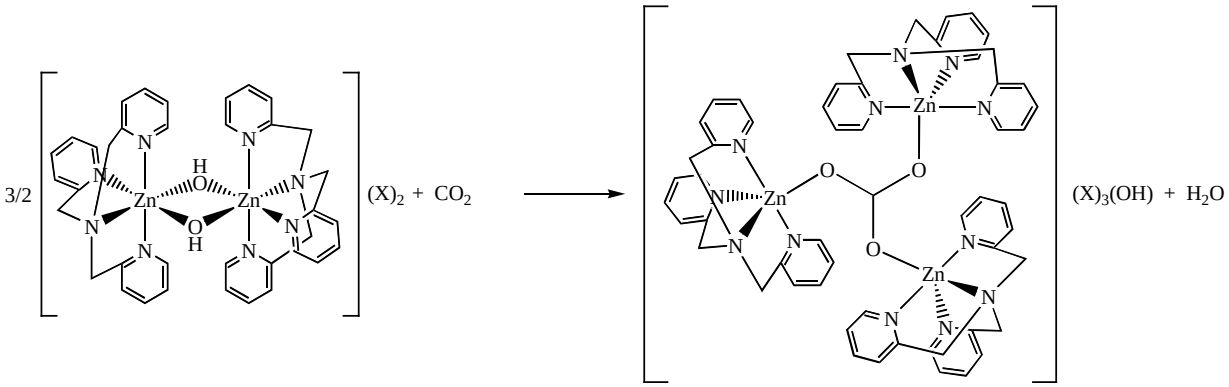

Scheme 2. Stoichiometric reaction of the Zn hydroxide dimer **1(X)$_2$** with CO_2 to give the trinuclear carbonate **2(X)$_3$(OH)** (X = ClO_4^- or NO_3^-)**.**

Titration of **1(NO$_3$)$_2$** with 1 M HCl in D_2O was monitored by ^{1}H NMR spectroscopy. Addition of aliquots of HCl gave no new product signals until 1.5 equiv HCl had been added. Addition of increasing amounts of HCl provided only one new set of signals, apart from small shifts of the original pyridyl H signals of **1(NO$_3$)$_2$**, consistent with the formation of [H$_x$NN3]Cl$_x$ (x = 3 or 4). After addition of 9 equiv HCl, nearly all **1(NO$_3$)$_2$** had been converted to [H$_x$NN3]Cl$_x$ and, since no precipitation was observed, (presumably) a soluble, hydrated Zn(II) salt. Given the lack of changes in the spectrum of **1(NO$_3$)$_2$** upon initial addition of acid the likely site for protonation is the hydroxy bridges (or the hydroxy ligand of a monomer) of **1(NO$_3$)$_2$**. This is consistent with the initial pH of the **1(NO$_3$)$_2$** solution of about 8.8 (see Figure S10) and the pK_a of 8.08 for $[(NN3)Zn(OH_2)]^{2+}$.[19] A similar experiment with **2(NO$_3$)$_4$** showed, after the first addition of HCl, nearly exact spectra to those obtained in the acid titration of **1(NO$_3$)$_2$**, suggesting loss of a $[(NN3)Zn]^{2+}$ moiety, followed

DOI: 10.1016/j.jcou.2017.02.007

by protonation at the carbonate bridge and loss of CO_2 to give the same $[(NN3)Zn(OH_2)]^{2+}$ species.

The similar behavior of **1(NO$_3$)$_2$** and **2(NO$_3$)$_4$**, the observation of only one new product, and the minor changes in the pyridyl-H resonances with decreasing pH are consistent with the presence of a rapid equilibrium between $[(NN3)Zn(OH)]^{+}$ and $[(NN3)Zn(OH_2)]^{2+}$. Selective irreversible dissociation and protonation of only one arm of the NN3 ligand would give rise to multiple signals from inequivalent pyridine moieties. For example, no selective protonation to de-coordinate one amino group in pentaamine Zn complex $[(Zn(pyN_4)(H_2O)]Br_2$ (pyN_4 = 2,6-$C_5H_3N[CMe(CH_2NH_2)_2]_2$) was observed.[20] It can thus be concluded that the NN3 ligand is completely labile after the eventual dissociation (protonation) of one N atom, and that $[(NN3)Zn(H_2O)]^{2+}$ and $[(NN3)Zn(OH)]^{+}$ are indistinguishable by ^{1}H NMR spectroscopy. The former conclusion is consistent with that observed in the potentiometric titrations of tren in the presence of $Zn(ClO_4)_2$,[21] and the latter is consistent with rapid proton addition to or loss from $[(NN3)Zn(OH)]^{+}$ or $[(NN3)Zn(H_2O)]^{2+}$ on the NMR time scale.[22] These results support the existence of a monomer-dimer equilibrium for **1(NO$_3$)$_2$** and a similar equilibrium after an acid-induced decarboxylation of **2(NO$_3$)$_4$.**

Since a PXRD pattern of the isolated trimer **2(NO$_3$)$_4$** was not consistent with the simulated PXRD pattern of **2(ClO$_4$)$_4$**, its structure was determined by a single crystal *X*-ray diffraction experiment (see Figure S2 in the Supplementary Material). The structure, which also contains a CH_3NO_2 molecule as a solvent of crystallization, is the expected trimer with a μ_3-κ^1,κ^1,κ^1 carboxylate ligand. The structure is, however, isomorphous with the Cu analogue $\{[(NN3)Cu]_3CO_3\}(ClO_4)_4$,[23] and not the known Zn structures **2(ClO$_4$)$_4$** and **2(ClO$_4$)$_4$•H$_2$O**.[23] While the metrical parameters of these four species are essentially the same (M-O distances 1.95-1.98 Å; M-N_{py}, 2.04-2.10 Å; M-N_{amine}, 2.20-2.26 Å), the distances of the metal atoms from the plane defined by the 4 atoms of the bridging carbonate ligand are different. In **2(NO$_3$)$_4$·CH$_3$NO$_2$** and $\{[(NN3)Cu]_3CO_3\}(ClO_4)_4$, two of the metal atoms are nearly coplanar with the carbonate plane, while the third is deviated significantly from the plane (0.556 Å for Zn03 in **2(NO$_3$)$_4$·CH$_3$NO$_2$**). For **2(ClO$_4$)$_4$** and **2(ClO$_4$)$_4$•H$_2$O**, two of the Zn atoms are located on one side of the carbonate plane (Zn-plane distance 0.23-0.35 Å), while the third Zn atom is on the other side of the carbonate plane at a distance of 0.66 Å.

The solid state ^{13}C NMR data for **2(NO$_3$)$_4$** are consistent with the XRD data in that there is no symmetry involving the three NN3 ligands, with the result of many distinct peaks in the

DOI: 10.1016/j.jcou.2017.02.007

spectrum, but only one carbonate peak at 169.3 ppm. Variable Hartmann-Hahn contact time experiments between 200 and 50 µs showed that, at a 75 µs contact time, the peak at 169.3 disappeared, the peaks between 155 to 160 ppm lost some intensity, and all other peaks kept their relative intensities (see Figure S3 in the Supplementary Material). This confirms that the C-atom resonating at 169.3 ppm has no bound protons and that the peaks at 155-160 ppm are the *ortho* C atoms of the pyridyl rings bound to the CH_2 moiety of the NN3 ligand. For comparison, the solid state ^{13}C signals for the carbonate C atom in the structurally related compound $\{[Zn([13]aneN_4)]_3CO_3\}(ClO_4)_4$ ([13]aneN$_4$ = 1,4,7,10-tetraazacyclotridecane)[24] and the 2D network structure $\{[Zn_3(L)_3(\mu\text{-}CO_3)](ClO_4)_4\cdot CH_3CN\}_n$ (L = bis(2-aminoethyl)(2-imidazolethyl)amine) [25] appear at 165 ppm and 167.9 ppm, respectively. The solid state ^{13}C chemical shifts for the carbonate C atom of the two bridging carbonate isomers $[\kappa^3\text{-Tptm}]Zn(\mu\text{-}\kappa^2,\kappa^1\text{-}OCO_2)Zn[\kappa^4\text{-Tptm}]$ and $[\kappa^4\text{-Tptm}]Zn(\mu\text{-}\kappa^2,\kappa^1\text{-}OCO_2)Zn[\kappa^4\text{-Tptm}]$ (Tptm = tris(2-pyridylthio)methyl) are 171.6 and 172.1 ppm.[26]

FT-ICR data were collected on methanol and aqueous solutions of both **1(NO$_3$)$_2$** and **2(NO$_3$)$_4$** (see Figures S9a-c in the Supplementary Material). The number of (NN3)Zn moieties present in the various fragments could be determined from the natural isotope pattern of Zn. Analyses of the aqueous solutions of both **1(NO$_3$)$_2$** and **2(NO$_3$)$_4$** showed fragments consistent with ions containing one, two and three (NN3)Zn moieties, in addition to various amounts of nitrate and hydroxide ions and coordinated water molecules. For **1(NO$_3$)$_2$**, the results indicate that the (NN3)Zn moiety stays intact throughout the ionization process but that rapid equilibria involving multinuclear species, even a trimeric $[Zn(NN3)]_3$ species, presumably with OH or OH_2 bridges, is present. In contrast, when using methanol as solvent, no fragments containing three (NN3)Zn groups were observed. This indicates that the solvent strongly affect the dynamics of the (NN3)Zn moiety, which again will affect the possible species formed in the reaction with dissolved CO_2 as described below.

In the FT-ICR-MS data from an aqueous solution of **2(NO$_3$)$_4$**, in the molecular weight range for monomeric fragments, three different species are observed: $(NN3)ZnO^+$ (M^+= 371 amu), $(NN3)ZnOCO^+$ (M^+= 399 amu) and $(NN3)ZnOCOOH^+$ (M^+= 416 amu). These correspond to fragments derived by splitting the central carbonate of the trimeric precursor at different points. Of these fragments, that with the highest abundance is the protonated carbonate species $(NN3)ZnOCOOH^+$.

3.2 Reaction of 1(NO$_3$)$_2$ with CO$_2$ in D$_2$O.

DOI: 10.1016/j.jcou.2017.02.007

Bubbling $^{13}CO_2$ through a solution of **1(NO$_3$)$_2$** for 5 minutes provided changes in the ^{13}C NMR spectrum, as shown in Figure 1. While there are only subtle changes in the ppm values for the carbon atoms of the NN3 ligands, two new signals appeared at 127.4 and 165.3 ppm. The former signal is due to dissolved $^{13}CO_2$, while the second signal is consistent with the formation of a carbonate species. Longer $^{13}CO_2$ bubbling times, up to 15 minutes, did not change the positions or intensities of these CO_2-derived signals. The observed peak at 165.3 ppm can be attributed to a carbonate C-atom in a metal carbonate species, or it can be from the peak arising from the uncoordinated HCO_3^-/CO_3^{2-} species in fast equilibrium. The limiting values for this equilibrium in water are 161.1 ppm (100% HCO_3^-) and 168.7 ppm (100% CO_3^{2-}), and depends upon the pH of the solution.[27] Therefore, this spectrum alone does not unambiguously assign the origin of the peak at 165.3 ppm. The change of the ^{13}C signals from the shift values attributed to **1(NO$_3$)$_2$** after adding CO_2 indicates that **1(NO$_3$)$_2$** is at least involved in an equilibrium with another, new species formed upon introduction of $^{13}CO_2$. This is different from the reaction of CO_2 with MEA, in which ^{13}C signals attributed to both MEA and its carbamate product are observed simultaneously, clearly indicating incomplete conversion and no equilibrium.[28] After correction for isotopic enrichment, the integrated areas

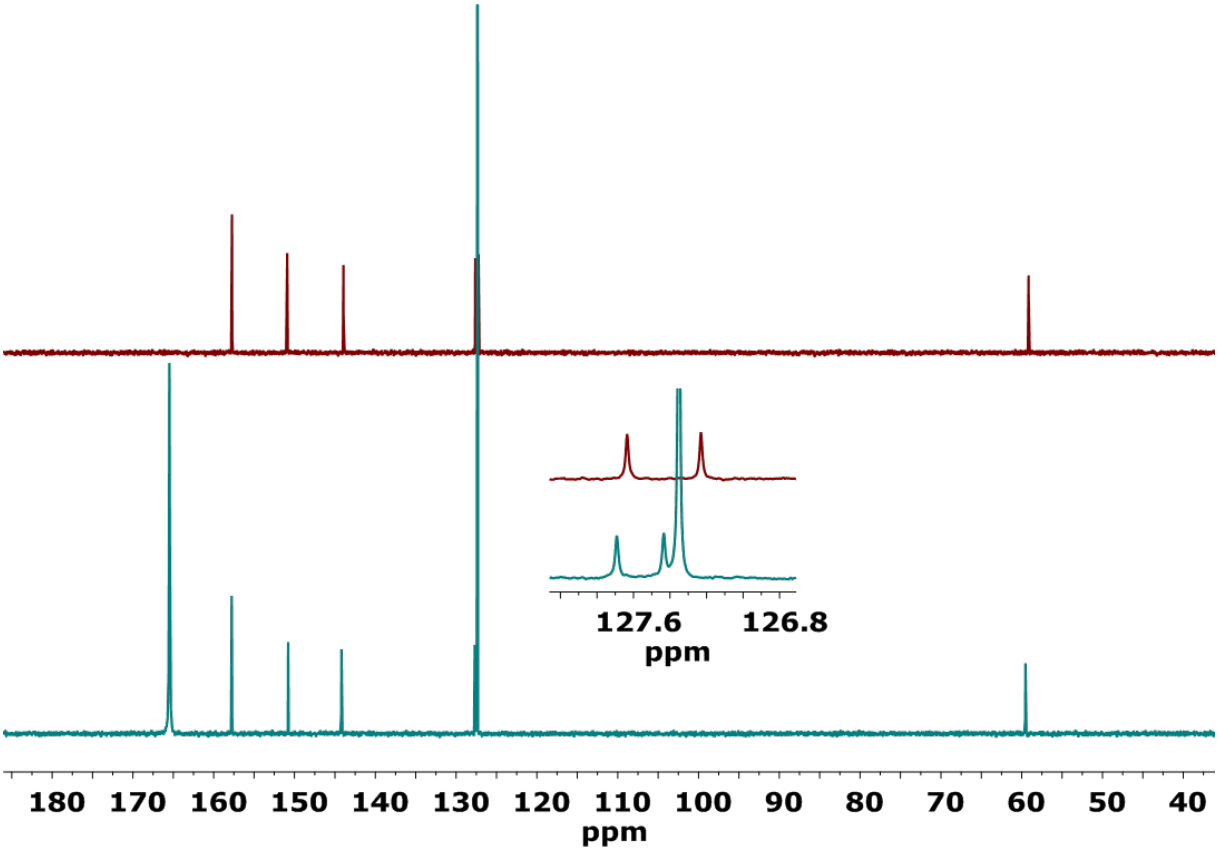

DOI: 10.1016/j.jcou.2017.02.007

Figure 1. Top: ^{13}C NMR spectrum of **1(NO$_3$)$_2$**. Bottom: ^{13}C NMR spectrum of **1(NO$_3$)$_2$** after bubbling $^{13}CO_2$ through the solution for 5 minutes. Inset shows the region between 126.8 and 128.0 ppm.

Table 1. Ratios of (NN3)Zn:CO_3^{2-} and (NN3)Zn:$CO_{2\,(aq)}$ after carboxylation and heating.

Sample	Ratio (NN3)Zn:CO_3^{2-}	Ratio (NN3)Zn:CO_2 (aq)
1(NO$_3$)$_2$ + CO_2	1.6:1	1.1:1
1(NO$_3$)$_2$ + CO_2, after heating to 85 °C	2.0:1	14:1
1(NO$_3$)$_2$ + CO_2, after heating to 85 °C and re-adding CO_2 at 25 °C	1.6:1	-
2(NO$_3$)$_4$ + CO_2	1.8:1	1.3:1
2(NO$_3$)$_4$ + CO_2, after heating to 85 °C	2.5:1	-
2(NO$_3$)$_4$ + CO_2, after heating to 85 °C and re-adding CO_2 at 25 °C	1.9:1	-
(**1(NO$_3$)$_2$ + 2(NO$_3$)$_4$**) + CO_2	1.6:1	1.1:1
(**1(NO$_3$)$_2$ + 2(NO$_3$)$_4$**) + CO_2, after heating to 85 °C	2.3:1	-

of the CH_2 signal at 60 ppm and the carbonate signal gave a (NN3)Zn:CO_3^{2-} ratio of 1.6; the corresponding ratio for (NN3)Zn:$CO_{2(aq)}$ (at 127 ppm) is 1.1 (see Table 1).

In order to characterize further the nature of the carbonate peak at 165.3 ppm, an EXSY experiment using a regular NOESY sequence with mixing time in a typical range for small molecule dynamics was performed. In Figure 2 clear cross peaks between dissolved CO_2 and the carbonate peak are observed. Since this is a proton-coupled spectrum, inequivalent doublets are observed for the *C*H atoms of the pyridyl moiety of the NN3 ligand.

If CO_2 is added to a water solution of the NN3 ligand, carbonate/bicarbonate is formed as expected for the reactivity of tertiary amines with CO_2.[29] An EXSY experiment on this reaction mixture does not provide any cross peaks involving CO_2 (not shown). This supports the assignment of the observed carbonate signal upon bubbling CO_2 through a solution of **1(NO$_3$)$_2$** as a metal-carbonate moiety and not simply a CO_3^{2-}/HCO_3^- equilibrium species. No

DOI: 10.1016/j.jcou.2017.02.007

^{67}Zn NMR spectrum could be obtained. This might be due to strong quadrupolar couplings, since the natural ^{67}Zn receptivity is approximately 70% that of ^{13}C.

In order to investigate the thermal stability of the products formed upon addition of CO_2 to aqueous solutions of **1(NO$_3$)$_2$**, the $^{13}CO_2$/**1(NO$_3$)$_2$** solution was heated to 85 °C for 1 hour and then cooled. The ^{13}C NMR spectra collected during this temperature program are presented in

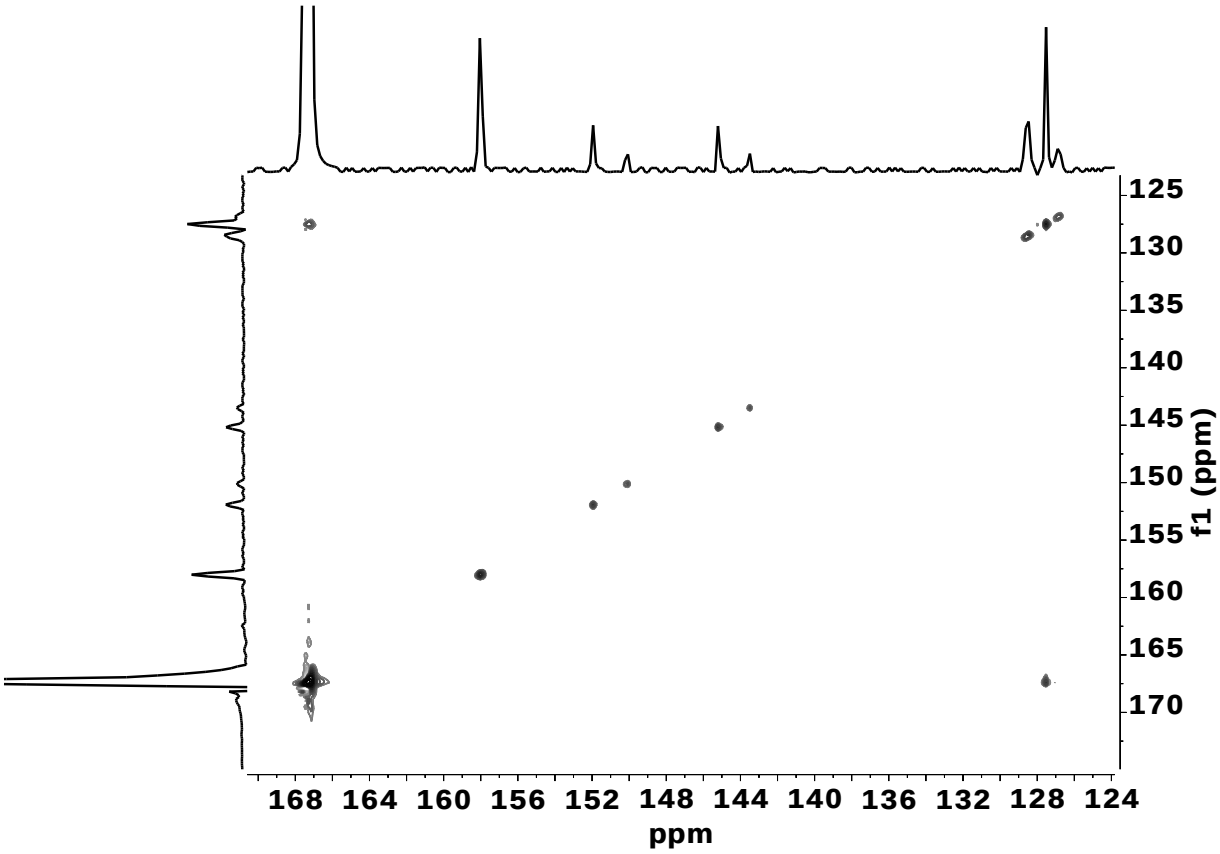

Figure 2. ^{13}C EXSY spectrum of the **1(NO$_3$)$_2$**/$^{13}CO_2$ system. This experiment was run after a heating cycle (vide infra), which is the reason for the low intensity of the $CO_{2\,(aq)}$ peak at 127 ppm.

Figure 3. Upon warming, the free $^{13}CO_2$ signal at 127.4 ppm broadened and lost intensity (undoubtedly due to diffusion out from the solution and not so much due to the temperature effect described by the Curie law). The observed broadening of the free $^{13}CO_2$ signal upon increasing temperature indicates that CO_2 could be undergoing exchange processes. Simultaneously, the carbonate signal at 165.3 ppm shifted to higher ppm values and split into at least two components that changed intensity after heating at 85 °C (see Figure 3, ppm range 167-169 ppm). The ^{13}C NMR signals of the NN3 ligands showed no such broadening or

DOI: 10.1016/j.jcou.2017.02.007

splitting, indicating that the $[(NN3)Zn]^{2+}$ moiety remains unaffected by the chemistry occurring during the heating process. The small shifts to higher ppm values for the ^{13}C peaks associated with the NN3 ligand are most likely due to temperature effects, as indicated by the analogous variation in chemical shifts with temperature observed upon heating only **1(NO$_3$)$_2$** in D_2O (See Figure S7 in the Supplementary Material). Upon cooling to 25 °C, the carbonate peak again coalesced into one signal. Neither the carbonate peak nor the NN3-derived signals had the same ppm shift values as those prior to heating, indicating their dependence on the

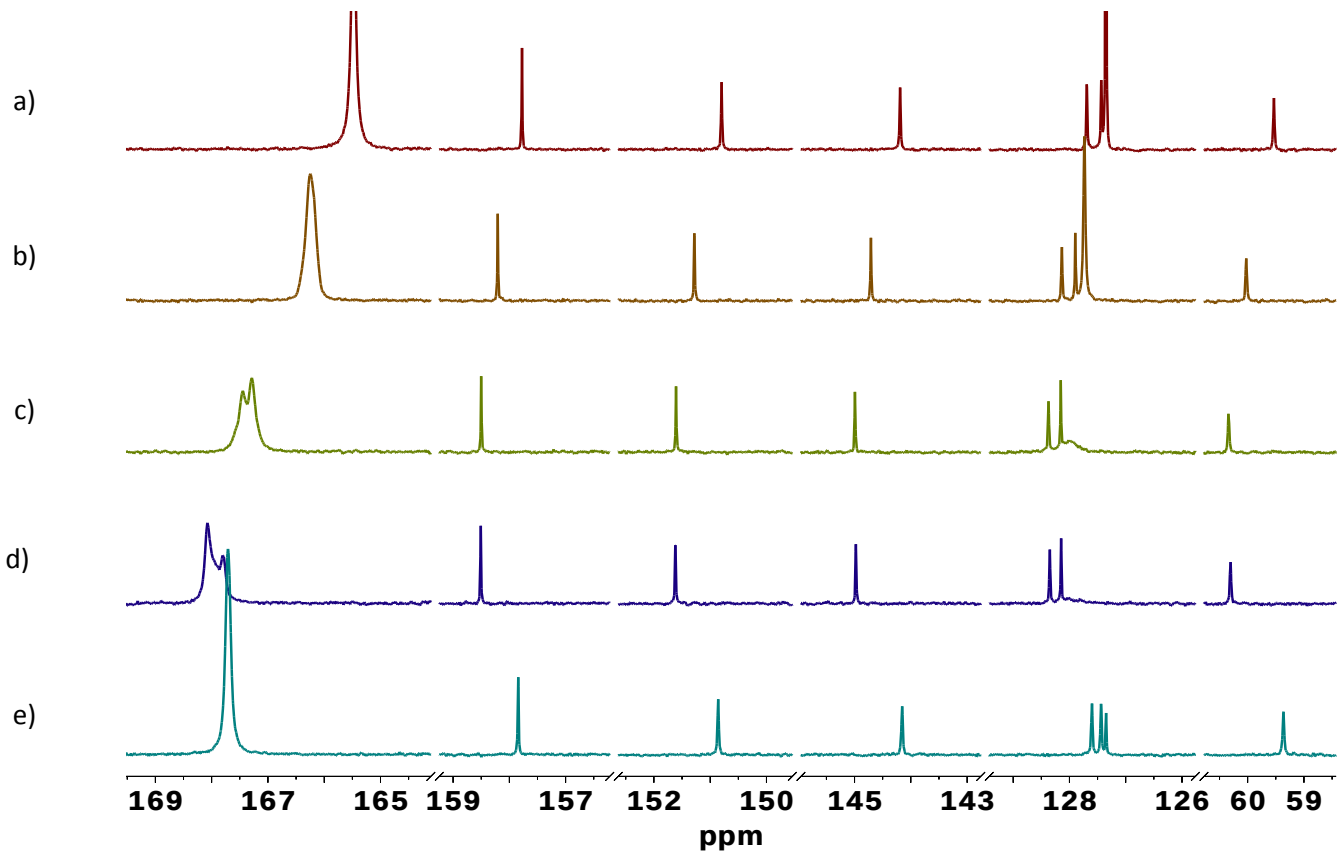

Figure 3. Stacked plot of ^{13}C NMR spectra from the heating of the $^{13}CO_2$/**1(NO$_3$)$_2$** to 85 °C and subsequent cooling. a) 25 °C, b) 60 °C, c) 85 °C, d) after 50 minutes at 85 °C, e) upon cooling to 25 °C. The sections of the abscissa without any peaks have been removed for clarity.

total CO_2 loading of the solution and the solution pH. In a separate experiment, the pH of an aqueous **1(NO$_3$)$_2$** solution (see Figure S10 in the Supplementary Material) was monitored under conditions corresponding to those used to obtain the spectra in Figure 3. A degassed ion-exchanged solution of **1(NO$_3$)$_2$** had an initial pH of 8.8 at 25 °C. With addition of CO_2, the pH dropped to 6.3. During heating to 85 °C, the pH steadily increased to 7.6 due to release of the dissolved CO_2, and the pH increased further to 7.8 upon cooling back to room temperature.

DOI: 10.1016/j.jcou.2017.02.007

The splitting and re-coalescence of the carbonate peak, in combination with the relatively static nature of the NN3 ^{13}C signals, strongly suggests that the single carbonate signal at 25 °C is representative of a fast exchanging system and not the formation of new stable chemical entities upon heating. The change in the position of the equilibrium carbonate peak is a result of the reduced concentration of one of the species due to loss of CO_2 in the system. The spectra in Figures 2 and 3 are therefore consistent with at least two equilibria in the **1(NO$_3$)$_2$**/$^{13}CO_2$ system, a relatively slow equilibrium involving CO_2 and a Zn-carbonate species (Figure 2) and a faster equilibrium between at least two Zn-carbonate species (Figure 3). Comparison of the two 25 °C spectra showed that the heating procedure reduced the intensities of the $CO_{2\,(aq)}$ and CO_3^{2-} peaks by 92% and 15%, respectively, corresponding to a total loss of about 36 % of the CO_2 and a (NN3)Zn:CO_3^{2-} ratio of 2:1. With an additional 5 minutes of CO_2 addition to the cooled solution (25 °C), the ^{13}C carbonate signal returned to 165 ppm and the (NN3)Zn:CO_3^{2-} ratio returned to 1.6, i.e. the same as after the initial CO_2 loading, indicating the reversibility of the system**.**

In a control experiment, $^{13}CO_2$ in pure D_2O was subjected to the same heating and cooling cycle (see Figure S8 in the Supplementary Material). Comparison of the two spectra recorded at 25 °C before and after heating showed that about 10% of the CO_2 remained in solution after cooling back to 25 °C. In addition no broadening of the CO_2 peak was observed at 85 °C, in contrast to what was observed for **1(NO$_3$)$_2$**/$^{13}CO_2$ (and also for **2(NO$_3$)$_4$**/$^{13}CO_2$, *vide infra*). This means that the peak broadening for the $^{13}CO_2$ signal in the presence of **1(NO$_3$)$_2$** is due to an exchange process involving the Zn-complex and not only due to higher temperature or transport out of the liquid.

3.3. Reaction of 2(NO$_3$)$_4$ with CO_2 in D_2O

Addition of CO_2 to a solution of **2(NO$_3$)$_4$** was performed similarly to that for **1(NO$_3$)$_2$**, and the ^{13}C NMR spectra of **2(NO$_3$)$_4$** and its carboxylation product are shown in Figure 4. Prior to the introduction of $^{13}CO_2$, the ^{13}C NMR spectrum of **2(NO$_3$)$_4$** showed, in addition to the carbon atoms of NN3, a peak at 169.4 ppm that is attributed to the CO_3 moiety in the molecule, consistent with that observed in the solid state spectrum of **2(NO$_3$)$_4$**, and outside the range of the HCO_3^-/CO_3^{2-} chemical shifts. The observed shift is consistent with the ^{13}C chemical shift of 168.5 ppm in D_2O for the carbonate carbon atom in the structurally analogous {[(tren)Zn]$_3$(μ_3-CO_3)](ClO$_4$)$_4$ (tren = tris(2-aminoethyl)amine).[30] The Zn coordination geometry in this species is, however, square pyramidal, as opposed to the

DOI: 10.1016/j.jcou.2017.02.007

trigonal bipyramidal geometry of the Zn atoms in **2(NO$_3$)$_4$**. Integration provided a (NN3)Zn:CO_3^{2-} ratio of 3.2, slightly more than that expected from the stoichiometry. This is likely due to the presence of some unreacted **1(NO$_3$)$_2$**. After CO_2 loading, new peaks were observed at 165.5 and 127.3 ppm. These ppm values are essentially the same as those observed after carboxylation of **1(NO$_3$)$_2$**, as the difference in ppm values for the two carbonate peaks is 0.02 ppm. Based upon these experiments, it is highly likely that there are one or more common end products after carboxylation of aqueous solutions of **1(NO$_3$)$_2$** and **2(NO$_3$)$_4$**, and that **2(NO$_3$)$_4$**, the observed thermodynamic (crystalline) product of **1(NO$_3$)$_2$** and CO_2 obtained in organic solvents, is not formed to any significant degree in carboxylated aqueous solutions. Upon carboxylation, the (NN3)Zn:CO_3^{2-} ratio decreased to 1.8, and the corresponding value for the (NN3)Zn:CO_2(aq) was 1.3.

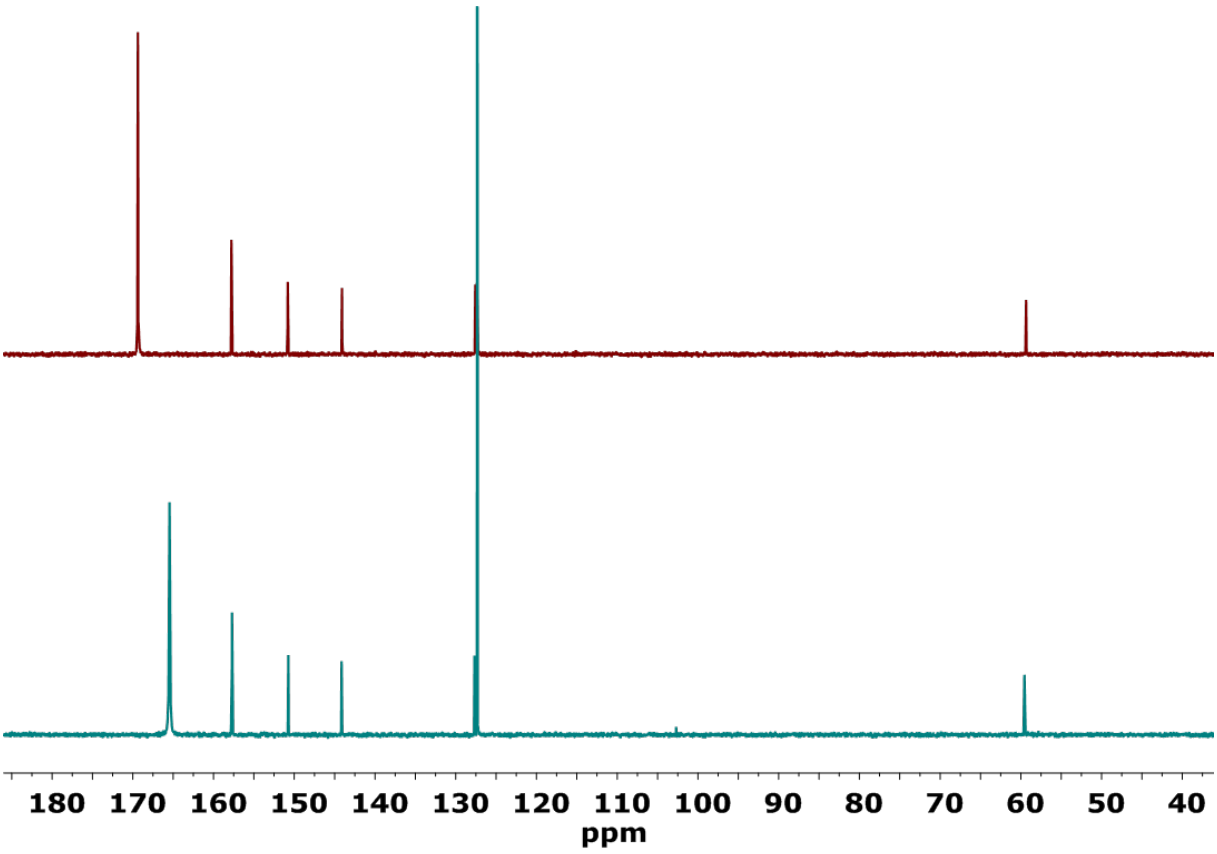

Figure 4. Top: ^{13}C NMR spectrum of **2(NO$_3$)$_4$**. Bottom: ^{13}C NMR spectrum of **2(NO$_3$)$_4$** after bubbling $^{13}CO_2$ through the solution for 5 minutes.

Heating the carboxylated solution of **2(NO$_3$)$_4$** to 85 °C and subsequently cooling back to 25 °C (Figure 5) showed many of the same features as observed for the **1(NO$_3$)$_2$**/$^{13}CO_2$ experiment, but with some key differences. As observed for the **1(NO$_3$)$_2$**/$^{13}CO_2$ system, the free $^{13}CO_2$ signal broadened and lost intensity during the heating cycle, and the carbonate

DOI: 10.1016/j.jcou.2017.02.007

peak at 165.5 ppm shifted to higher ppm values and split into at least two components, only to coalescence again upon cooling. In contrast, the peaks of the NN3 carbon atoms in **2(NO$_3$)$_4$** split into two peaks at 85 °C, indicating the presence of two inequivalent and nonequilibrating (on the NMR time scale) [(NN3)Zn]$^{2+}$ moieties at this temperature.

The CO_2 and carbonate peak intensities were reduced by 94% and 22%, respectively, during the heating to 85 ºC. The integrations of these signals upon cooling indicated that 43 % of the added $^{13}CO_2$ was lost during the temperature cycle and that the (NN3)Zn:CO_3^{2-} ratio had

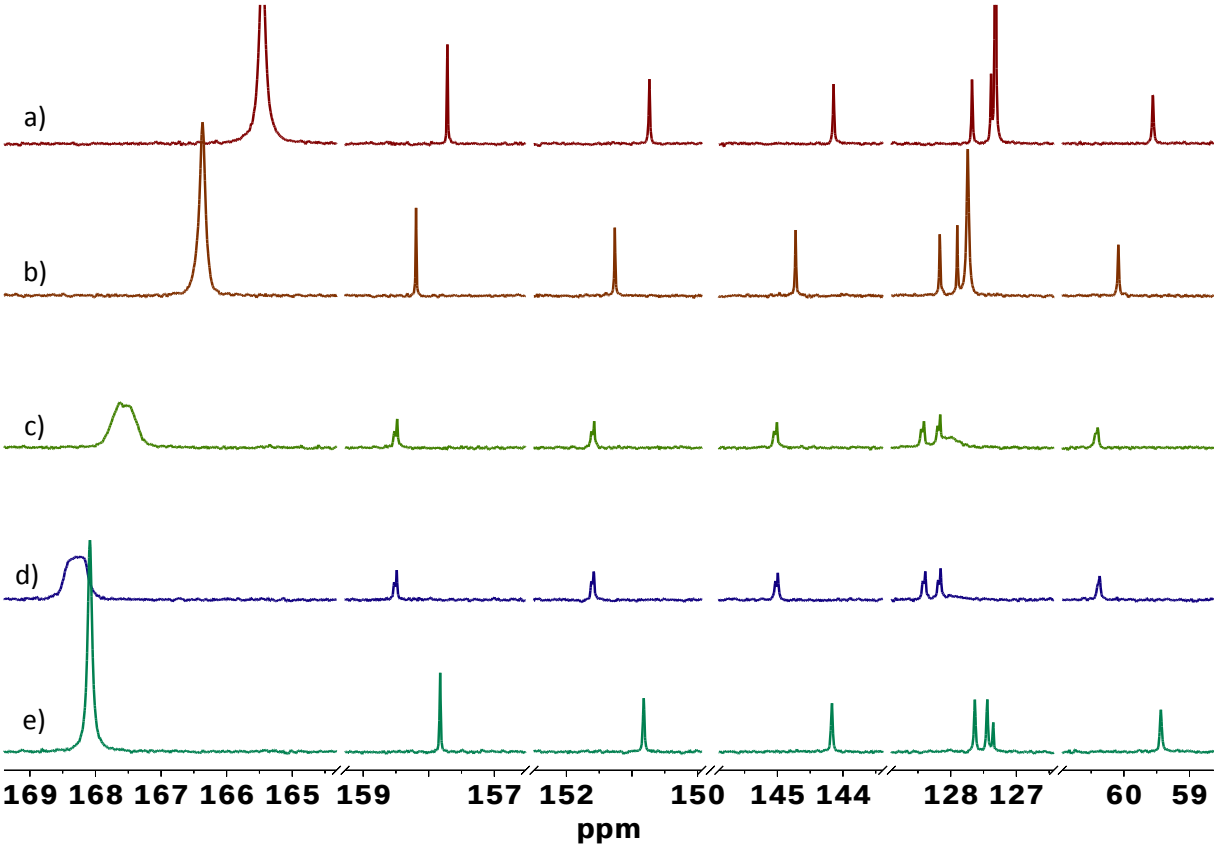

Figure 5. Stacked plot of ^{13}C NMR spectra from the heating of the **2(NO$_3$)$_4$**/$^{13}CO_2$ to 85 °C and subsequent cooling. a) 25 °C, b) 60 °C, c) 85 °C, d) after 50 minutes at 85 °C, e) upon cooling to 25 °C. The sections of the abscissa without any peaks have been removed for clarity.

increased to 2.5. With an additional 5 minutes of CO_2 loading to this solution after cooling to 25 °C (spectrum not shown), the (NN3)Zn:CO_3^{2-} ratio returned to 1.9, i.e. nearly the same as the 1.8 ratio observed after the initial CO_2 loading.

The pH of an aqueous **2(NO$_3$)$_4$** solution was also was monitored under conditions corresponding to those used for the NMR investigation (see Figure S10 of the Supplementary Material). The starting pH of 8.1 for the **2(NO$_3$)$_4$** solution was lower that for **1(NO$_3$)$_2$**,

DOI: 10.1016/j.jcou.2017.02.007

however, solutions **1(NO$_3$)$_2$** and **2(NO$_3$)$_4$** gave nearly identical pH values upon the addition of CO_2 to the solution and the subsequent heating and cooling cycle. The starting pH of the **2(NO$_3$)$_4$** solution is nearly identical to the pK_a of $[(NN3)Zn(OH_2)]^{2+}$.

3.4. Reaction of mixed 1(NO$_3$)$_2$ and 2(NO$_3$)$_4$ with CO$_2$ in D$_2$O

Mixing D_2O solutions of **1(NO$_3$)$_2$** and **2(NO$_3$)$_4$** containing equal moles of the (NN3)Zn moiety gave a ^{13}C spectrum with only one set of signals for the NN3 ligands and a single carbonate signal at 170.0 ppm, rather than a superposition of the individual spectra. The positions of the ^{13}C signals arising from the NN3 ligands in the combined solution were intermediate between the signals for **1(NO$_3$)$_2$** and **2(NO$_3$)$_4$**. This indicates a rapid equilibrium, exchanging all the (NN3)Zn moieties. The (NN3)Zn:CO_3^{2-} ratio was 6.5, consistent with the addition of excess (NN3)Zn via **2(NO$_3$)$_4$**. Heating this combined solution to 85 °C and subsequent cooling showed no evidence of peak splitting, peak broadening or decomposition.

Carboxylation of the combined solution via bubbling of $^{13}CO_2$ for 5 minutes gave a (NN3)Zn:CO_3^{2-} ratio of 1.6 and a (NN3)Zn:CO_2(aq) ratio of 1.1, similar to the results from the carboxylation of **1(NO$_3$)$_2$** (Figure 2). Subsequent heating to 85 °C provided spectra similar to that observed for **1(NO$_3$)$_2$** alone; there was no peak splitting of the NN3 ligands signals as observed for **2(NO$_3$)$_4$** in Figure 5. After cooling the (NN3)Zn:CO_3^{2-} ratio was estimated to be 2.3.

3.5. Comparison of ^{13}C NMR chemical shifts

There is apparently only one publication providing the ^{13}C chemical shifts in water for a carbonic anhydrase mimic or a trimeric Zn carbonate system analogous to that presented here, the aforementioned $\{[(tren)Zn]_3(\mu_3\text{-}CO_3)](ClO_4)_4$.[29] In addition to the chemical shift of the carbonate C atom this complex, the change in the ^{13}C chemical shift of the carbonate signal in the $[Zn(tren)(H_2O)](ClO_4)_2$ + excess $NaH^{13}CO_3$ system was monitored as a function of pH. In the slightly basic pH range 8-11, two peaks were observed, a strong signal assigned to the HCO_3^-/CO_3^{2-} equilibrium and a second, weaker multiplet between 167.5-167.7 ppm, which was assigned to different, but uncharacterized, Zn carbonate species.

The other ^{13}C chemical shifts for various carbonate species are reported in deuterated organic solvents, which makes a direct comparison with the shifts reported herein in aqueous media less precise. Not only are solvent effects included, but the HCO_3^-/CO_3^{2-} equilibrium will also

DOI: 10.1016/j.jcou.2017.02.007

be inoperative. For example, the ^{13}C chemical shift of the [κ^3-Tptm]Zn(μ-κ^2,κ^1-OCO_2)Zn[κ^4-Tptm] and [κ^4-Tptm]Zn(μ-κ^2,κ^1-OCO_2)Zn[κ^4-Tptm] equilibrium is 170.7 ppm in CD_2Cl_2,[26] while the carbonate carbon atom of [Zn(phen)$_2$(μ_2-CO_3)]•7H_2O resonates at 171.1 ppm in C_2D_5OD[31] and that of {[η^3-HB(3-Bu^t-5-Mepz)$_3$]Zn}$_2$(μ,η^1,η^1-CO_3) resonates at 164.0 ppm in C_6D_6.[32] The carbonate carbon of monodentate Zn bicarbonate species resonates at lower ppm values, such as that for [Zn(tnpa)(HCO_3)](ClO_4) (tnpa = tris(6-neopentylamino-2-pyridylmethyl)amine) at 160.84 ppm in CD_3OD.[33]

3.6. Mechanistic considerations and their relation to CO_2 desorption

A mechanistic scheme consistent with the observations is presented in Scheme 3. All the results indicate that, in aqueous solutions, both **1(NO$_3$)$_2$** and **2(NO$_3$)$_4$** are labile species and capable of forming monomeric, dimeric and trimeric species. This is shown by the FT-ICR data as well as the inability to detect both **1(NO$_3$)$_2$** and **2(NO$_3$)$_4$** as distinct entities in a combined aqueous solution. The equivalency of all the NN3 C atoms upon mixing solutions of **1(NO$_3$)$_2$** and **2(NO$_3$)$_4$** illustrates that all [(NN3)Zn]$^{2+}$ moieties of **2(NO$_3$)$_4$** undergo rapid exchange through the loss of the formally datively bound [(NN3)Zn]$^{2+}$ group. As well, the data show that the [(NN3)Zn]$^{2+}$ moiety stays intact under all transformations.

Starting from **1(NO$_3$)$_2$**, carboxylation provides an equilibrium mixture of species **A** and **B** (or **B'**), which are a monomeric Zn-hydrogen carbonate species and a μ_2-κ^1, κ^1-carbonate-bridged Zn dimer, respectively. The steps leading to the formation of species **A** and **B** are well established in other Zn systems, and this mechanism has been proposed previously.[29] The detection of the monomeric carbonate **A** in the FT-ICR-MS data support its involvement in the reaction. Some of the individual steps of this part of the proposed mechanism have also been previously studied. For example, the insertion of CO_2 into the Zn-OH bond of [Tp$^{t\text{-}Bu,Me}$]ZnOH (Tp$^{t\text{-}Bu,Me}$ = tris(3-t-butyl-5-methylpyrazolyl)hydroborate) species[34] has been observed by low temperature ^1H and ^{13}C NMR, and the reversibility of the CO_2 insertion into Zn-OH bonds is well-established.[31] The rapid combination of a monodentate metal bicarbonate and a monomeric metal hydroxide (or metal aquo species) to give dimers such as **B** has also been proposed on a number of occasions.[29,31,35] The observed (NN3)Zn:CO_3^{2-} ratio of 1.6 is consistent with a 2:3 ratio of **A**:**B**.

DOI: 10.1016/j.jcou.2017.02.007

Monodentate metal bicarbonate and carbonate species have been observed to be more prone to hydrolysis than the corresponding bidentate species,[36] suggesting that **B'** may actually be the dominant dimer species in solution. Formation of both a η^1, η^1-carbonate Zn dimer and a η^1, η^2-carbonate Zn dimer has also been shown in pyrazoylborate systems.[32] However, both **A**, and therefore **B** (as an intermediate between **A** and **B'**), must be present in solution in order to facilitate the observed exchange between the equilibrated Zn-carbonate species and free CO_2, when starting from **1(NO$_3$)$_2$**. A reasonable supposition therefore is that the ^{13}C carbonate peak at 165.5 ppm observed upon carboxylation of **1(NO$_3$)$_2$** is an equilibrium mixture of **A** and **B** (or **A**, **B**, and **B'**). After heating and CO_2 loss from that dissolved in the solution and through **A**, the lower CO_2 loading (higher relative concentration of (NN3)Zn) increases the amount of **B** (or **B'**) relative to **A** and provides an observed shift in the carbonate signal to higher ppm values.

Dissolution of **2(NO$_3$)$_4$** gives a ^{13}C carbonate signal nearly identical to that observed in the solid state spectrum, strongly suggesting that **2(NO$_3$)$_4$** is more or less intact in solution. However, the observed equivalence of all the (NN3)Zn moieties upon dissolution of both **1(NO$_3$)$_2$** and **2(NO$_3$)$_4$** indicates that there is some degree of $[(NN3)Zn]^{2+}$ dissociation. The pH of the **2(NO$_3$)$_4$** solution is essentially that of the pK_a for $[(NN3)Zn(H_2O)]^{2+}$, indicating that around 50 % of any dissociated $[(NN3)Zn]^{2+}$ species is in the aqueous (as opposed to hydroxide) form. The concentration of $[(NN3)Zn(H_2O)]^{2+}$ will actually increase upon carboxylation, due to the lower pH. This difference between the two complexes, that **2(NO$_3$)$_4$** provides some $[(NN3)Zn(H_2O)]^{2+}$ that will not react with CO_2, while **1(NO$_3$)$_2$** does not, is significant for the explanation of the spectral differences observed upon carboxylation and heating of the two complexes. Carboxylation of the **2(NO$_3$)$_4$** solution still drives the complex into the same **A**-**B**-**B'** equilibrium as **1(NO$_3$)$_2$**, as indicated by the (nearly) identical ^{13}C spectra, but with non-carboxylated [(NN3)Zn] moieties, as indicated by the larger (NN3)Zn:CO_3^{2-} ratio for **2(NO$_3$)$_4$** as opposed to **1(NO$_3$)$_2$** (see Table 1). Even though they are not carboxylated, the $[(NN3)Zn(H_2O)]^{2+}$ species can still be involved in the equilibrium with the carbonates. As long as there is some **B** in solution, coordination of $[(NN3)Zn(H_2O)]^{2+}$ to the free O atom of the carbonate provides a route that can give rise to equivalent (NN3)Zn moieties.

The evidence strongly suggests inclusion of **A** in all the observed equilibria as necessary to explain the observed, relatively slow interconversion between all equilibrated carbonate species and CO_2, as proven by the cross-peak in Figure 2. Indeed, the literature clearly

DOI: 10.1016/j.jcou.2017.02.007

indicates that a species such as **A** is the only avenue for such an interconversion and the absorption or desorption of CO_2. For this reason, it is proposed that formation of **A** via hydrolysis from **B** is, in this system, an uphill process, such that the concentration of **A** increases with increasing temperature. Invocation of **A** as the species favored at higher temperature also explains the presence of the two sets of NN3 signals upon heating a carboxylated solution of **2(NO$_3$)$_4$**. Specifically, as stated above, carboxylation of **2(NO$_3$)$_4$** gives rise to $[(NN3)Zn(H_2O)]^{2+}$ species not formed in the carboxylation of **1(NO$_3$)$_2$**. The $[(NN3)Zn]^{2+}$ fragments of the aqua dication cannot equilibrate with those of **A**, as water dissociation is presumably a disfavored process in diluted aqueous solution.

DOI: 10.1016/j.jcou.2017.02.007

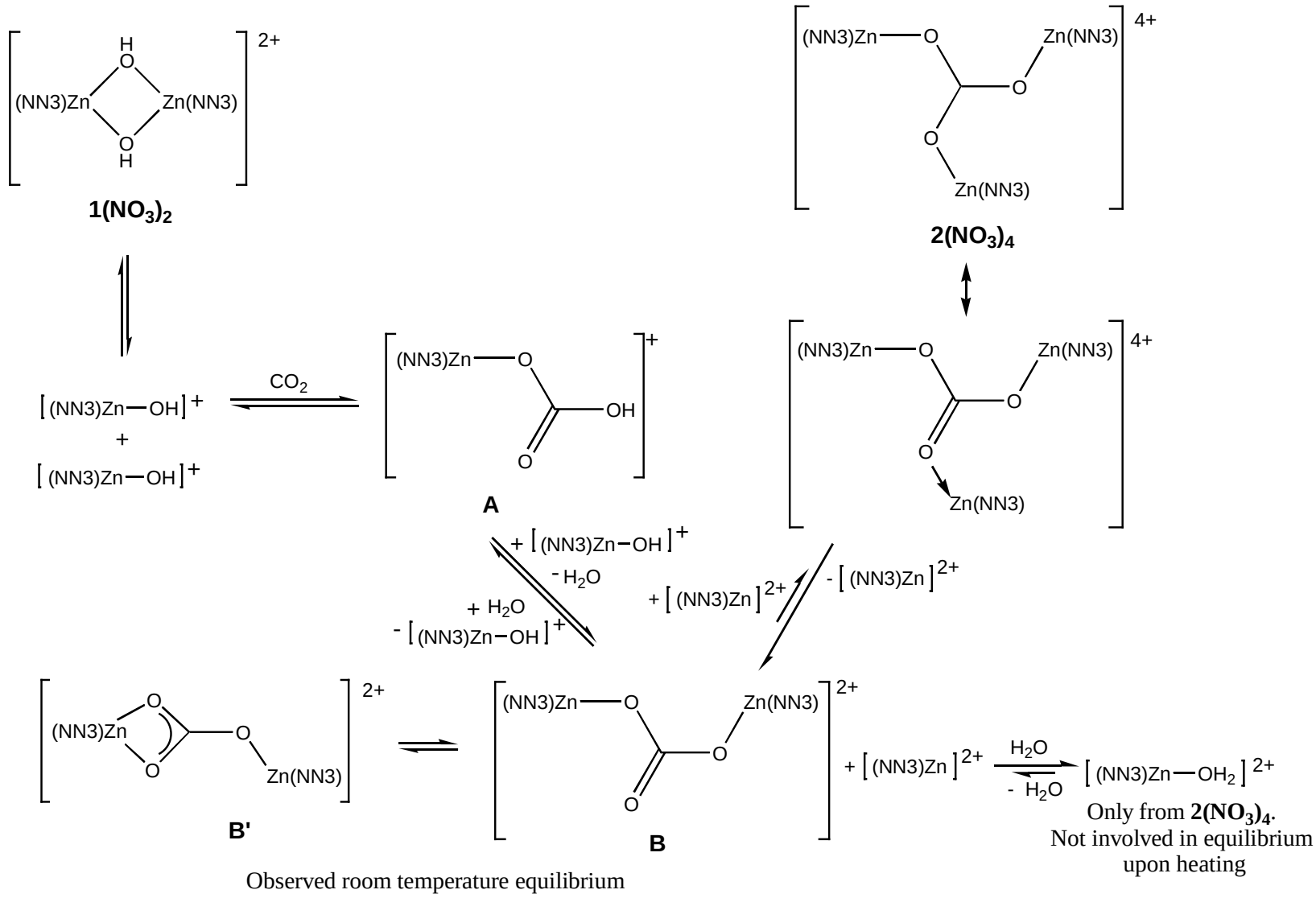

Scheme 3. Mechanistic proposal for the carboxylation of **1(NO$_3$)$_2$** and **2(NO$_3$)$_4$** in H_2O.

DOI: 10.1016/j.jcou.2017.02.007

4. Summary

A tris(pyridyl)amine-complexed zinc hydroxide dimer, **1(NO$_3$)$_2$**, has a coordination sphere that loosely resembles carbonic anhydrase and reacts with atmospheric CO_2 to give the trimetallic carbonate **2(NO$_3$)$_4$** as the isolable product. These properties suggest that **1(NO$_3$)$_2$** could have potential to act as a new "solvent" for a post-combustion capture process. While the absorption capacities and kinetics of **1(NO$_3$)$_2$** have been investigated,[14] a better understanding of the mechanism of absorption and desorption and the degree of involvement of the (presumed) thermodynamic carboxylation product **2(NO$_3$)$_4$** was desired. Therefore, an investigation of the carboxylation-decarboxylation processes of both **1(NO$_3$)$_2$** and **2(NO$_3$)$_4$** employing primarily ^{13}C NMR spectroscopy was undertaken. The data strongly support a mechanism whereby the primary reaction manifold arises from a monomeric Zn carbonate $[(NN3)ZnOCO_2H]^+$ and one or more forms of a dimeric Zn carbonate $[(NN3)ZnOCO_2Zn(NN3)]^{2+}$. Decarboxylation is proposed to proceed exclusively through the monomeric carbonate, which is the higher energy species. While both the monomeric and dimeric carbonates have precedent in the literature, their structures and reactivities are primarily based on non-aqueous chemistry. While **2(NO$_3$)$_4$** is the isolable product from the carboxylation of **1(NO$_3$)$_2$** in organic solvents, there is no evidence for its involvement in the carboxylation-decarboxylation processes in aqueous solution. Rather, the spectroscopic data of **2(NO$_3$)$_4$** differentiates itself through the presence of an additional and partially unreactive $[(NN3)Zn(OH_2)]^{2+}$ moiety that is not present when **1(NO$_3$)$_2$** is the starting material.

This is the first attempt, to our knowledge, to study the actual carboxylation chemistry of simple molecular CA mimics in aqueous solutions. While the ability of **1(NO$_3$)$_2$** and similar complexes to react with low partial pressures of CO_2 make them interesting candidates for a new type of CO_2 sorbent, this reactivity does not ensure lower desorption temperatures as compared to the current state-of-the-art. Modification of the ligand set to better balance the trade-off between reaction with low partial pressures of CO_2 and improvement of the desorption kinetics, or studies to assess the catalytic potential of **1(NO$_3$)$_2$** or its analogues in CO_2 capture processes, may be fruitful avenues of further investigation.

Supplementary material. X-ray experimental description and crystal data, data collection and refinement parameter table for **2(NO$_3$)$_4$·CH$_3$NO$_2$**, experimental details of the solid state NMR experiments, FT-ICR analyses, and pH measurements. Figures of the ^1H NMR spectra for the titration of **1(NO$_3$)$_2$** with 1 M HCl; ORTEP of **2(NO$_3$)$_4$·CH$_3$NO$_2$**; ^1H-^{13}C cross

DOI: 10.1016/j.jcou.2017.02.007

polarization (CP) solid state NMR spectra of **2(NO$_3$)$_4$** with viable H-H contact time; ^{1}H and ^{13}C NMR spectra of the ligand NN3 in D_2O; ^{1}H and ^{13}C NMR spectra of **1(NO$_3$)$_2$** in D_2O; ^{1}H and ^{13}C NMR spectra of **2(NO$_3$)$_4$** in D_2O; variable temperature spectra of **1(NO$_3$)$_2$** in D_2O; FT-ICR spectra for **1(NO$_3$)$_2$** and **2(NO$_3$)$_4$** in both H_2O and MeOH; variable temperature pH values of both **1(NO$_3$)$_2$** and **2(NO$_3$)$_4$** in the presence of CO_2.

Acknowledgements. We would like to thank the Research Council of Norway and Statoil ASA for financial support from project 224883/E20. We would also like to thank Dr. Anna Lind for recording the PXRD data and Dr. Anna Nordborg and Dr. Sven Even Borgos for performing the FT-ICR experiments.

DOI: 10.1016/j.jcou.2017.02.007

References

[1] Boot-Handford, M. E.; Abanades, J. C.; Anthony, E. J.; Blunt, M. J.; Brandani, S.; Mac Dowell, N.; Fernandez, J. R.; Ferrari, M.-C.; Gross, R.; Hallett, J. P.; Haszeldine, R. S.;Heptonstall, P.; Lyngfelt, A.; Makuch, Z.; Mangano, E.; Porter, R. T. J.; Pourkashanian, M.; Rochelle, G. T.; Shah, N.; Yao, J. G.; Fennell, P. S. *Energy Environ. Sci*., **2014**, *7*, 130-189.

[2] Gouedard, C.; Picq, D.; Launay, F.; Carrette, P. L., *Int. J. Greenhouse Gas Control* **2012**, *10*, 244-270; Sharma, S. D.; Azzi, M. *Fuel*, **2014**; *121*: 178-188

[3] Liang, Z., Rongwong, W., Liu, H., Fu, K., Gao, H., Cao, F., Zhang, R., Sema, T., Henni, A., Sumon, K., Nath, D., Gelowitz, D., Srisang, W., Saiwan, C., Benamor, A., Al-Marri, M., Shi, H., Supap, T., Chan, C., Zhou, Q., Abu-Zahra, M., Wilson, M., Olson, W., Idem, R., Tontiwachwuthikul, P. *Int. J. Greenhouse Gas Contr.* **2015**, *40*, 26-54.

[4] Lu, Y.; Ye, X.; Zhang, Z.; Khodayari, A.; Djukadi, T., *Energy Procedia* **2011**, *4*, 1286-1293;

[5] Merle, G.; Fradette, A.; Madore, E.; Barralet, J. E. *Langmuir* **2014**, *30*, 6915-6919.

[6] Yong, J. K. J.; Stevens, G. W.; Caruso, F.; Kentish, S. F. *J. Chem. Technol. Biotechnol.* **2015**, *90*, 3-10.

[7] (a) Davy, R. *Energy Procedia* **2009**, *1*, 885-892. (b) Davy, R.; Shanks, R. A.; Periasamy, S.; Gustafason, M. P.; Zambergs, B. M. *Energy Procedia* **2011**, *4*, 1691-1698.

[8] Koziol, L.; Valdez, C. A.; Baker, S. E.; Lau, E. Y.; Floyd, W. C., III, Wong, S. E.; Satcher, J. H., Jr.; Lightstone, F. C.; Aines, R. D. *Inorg. Chem.* **2012**, *51*, 6803-6812.

[9] Floyd, W. C., III; Baker, S. E.; Valdez, C. A.; Stolaroff, J. K.; Bearinger, J. P.; Satcher, J. H., Jr.; Aines, R. D. *Environ. Sci. Tech.* **2013**, *47*, 10049-10055.

[10] Recent examples of each bonding mode: Mode A: Jamali, S.; Milić, D.; Kia, R.; Mazloomi, Z.; Abdolahi, H. *Dalton Trans.* **2011**, *40*, 9362-9365. Mode B: Nadna, P. K.; Bera, M.; Aromí, G.; Ray, D. *Polyhedron*, **2006**, *25*, 2791-2799. Mode C: Zhang, J.; Yang, Q.; Zhu, Y.; Liu, H.; Chi, Z.; Su, C.-Y. *Dalton Trans.* **2014**, *43*, 15785-15790. Mode D: Naskar, J. P.; Drew, M. G. B.; Hulme, A.; Tocher, D. A.; Datta, D. *CrystEngComm* **2005**, *7*, 67-70. Mode E: Du, L.; Zhang, S.; Ding, Y. *Z. Anorg. Allg. Chem.* **2012**, *638*, 1039-1041. Mode F: Khan, S.; Roy, S.; Bhar, K.; Kumar, R. K.; Maji, T. K.; Ghosh, B. K. *Polyhedron* **2012**, *32*, 54-59. Mode G: Craig, G. A.; Roubeau, O.; Ribas-Ariño, Teat, S. J.; Aromí, G. *Polyhedron* **2013**, *52*, 1369-1374. Mode H: Bag, P.; Dutta, S.; Biswas, P.; Maji,

DOI: 10.1016/j.jcou.2017.02.007

S. K.; Flörke, U.; Nag, K. *Dalton Trans.* **2012**, *41*, 3414-3423. Mode I*:* Fondo, M.; García-Deibe, A. M.; Ocampo, N.; Sanmartín, J.; Bermejo, M. R. *Dalton Trans.* **2004**, 2135-2141.

[11] (a) Ke, H.; Zhao, L.; Xu, G.-F.; Guo, Y.-N.; Tang, J.; Zhang, X.-Y.; Zhang, H.-J. *Dalton Trans.* **2009**, 10609-10613. (b) Jiang, Y.; Wang, X.; Ying, X.; Zhong, F.; Cia, J.; He, K. *Inorg. Chem. Commun.* **2006**, *9*, 1063-1066.

[12] No examples of reaction with NO_x to give a Zn-nitrite or nitrate complex could be found. Only one example of the reaction of SO_x to form a Zn-sulfite or sulfate complex was found, specifically the insertion of SO_2 into a Zn-OH bond. Ruf. M.; Vahrenkamp, H. *Inorg. Chem.* **1996**, *35*, 6571-6578.

[13] Murthy, N. N.; Karlin, K. D. *J. Chem. Soc., Chem. Commun.* **1993**, 1236-1238.

[14] A balanced reaction for the carboxylation of **1(NO$_3$)$_2$** gives the product as **2(NO$_3$)$_3$(OH)**. The structurally characterized compound has the formula **2(NO$_3$)$_4$.** While the structural formulation may not represent the actual anion distribution in solution, it will be used throughout the text for simplicity.

[15] Heyn, R. H.; Aronu, U. E.; Vevelstad, S. J.; Hoff, K. A.; Didriksen, T.; Arstad, B.; Blom, R. *Energy Proc.* **2014**, *63*, 1805-1810.

[16] Gafford, B. G.; Holwerda, R. A. *Inorg. Chem.* **1989**, *28*, 60-66.

[17] Harris, R.K. ; Becker, E. D.; Cabral de Menezes, S. M.; Goodfellow, R.; Granger, P.; *NMR Nomenclature: Nuclear Spin Properties and Conventions for Chemical Shifts. IUPAC Recommendations 2001.* Sol.St.Nuc.Mag. Res. **2002,** *22*, 458-483.

[18] Long, J. R., *Chem. Health Safety* **2002**, *9*, 12-18

[19] Mareque-Rivas, J. C.; Prabaharan, R.; de Rosales, R. T. *Chem. Commun.* **2004**, 76-77

[20] López, J. P.; Heinemann, F. W.; Grohmann, A. *Z. Naturforsch.* **2004**, *59b*, 1600-1604.

[21] Canary, J. W.; Xu, J.; Castagnetto, J. M.; Rentzeperis, D.; Marky, L. A. *J. Am. Chem. Soc.* **1995**, *117*, 11545-11547.

[22] Bergquist, C.; Fillebeen, T.; Morlok, M. M.; Parkin, G. J. Am. Chem. Soc. 2003, 125, 6189-6199.

[23] Yan, S.; Cui, J.; Liu, X.; Cheng, P.; Liao, D.; Jiang, Z.; Wang, G.; Wang, H.; Yao, X. Sci. China, Ser. B, Chem. **1999**, *42*, 535-542.

[24] Notni, J.; Schenk, S.; Görls, H.; Breitzke, H.; Anders, E. *Inorg. Chem.* **2008**, *47*, 1382-1390

[25] Kong, L.-Y.; Zhang, Z.-H.; Zhu, H.-F.; Kawaguchi, H.; Okamura, T.; Doi, M.; Chu, A.; Sun, W.-Y.; Ueyama, N. *Angew. Chem. Int. Ed.* **2005**, *44*, 4352-4355.

DOI: 10.1016/j.jcou.2017.02.007

[26] Sattler, W.; Parkin, G. *Chem. Sci.***2012**, *3*, 2015-2019.

[27] Perinu, C.; Arstad, B.; Bouzga, A. M.; Svendsen, J. A.; Jens, K. J. *Ind.Eng.Chem.Res.* **2014**, *53*, 14571-14578.

[28] Perinu, C.; Arstad, B.; Bouzga, A. M.; Jens, K. J. *J.Phys.Chem. B* **2014**, *118*, 10167-10174.

[29] Donaldson, T.L.; Nguyen, Y.N. 1980. *Ind. Eng. Chem. Fund*. **1980**, *19*, 260–266.

[30] Mao, Z.-W.; Liehr, G.; van Eldik, R. *J. Chem. Soc. Dalton Trans.* **2001**, 1593-1600.

[31] Erras-Hanauer, H.; Mao, Z.-W.; Liehr, G.; Clark, T.; van Eldik, R. *Eur. J. Inorg. Chem.* **2003**, 1562-1569.

[32] Looney, A.; Han, R.; McNeill, K.; Parkin, G. *J. Am. Chem. Soc*. **1993**, *115*, 4690-4697.

[33] Yamaguchi, S.; Tokairin, I.; Wakita, Y.; Funahashi, Y.; Jitsukawa, K. Masuda, H. *Chem. Lett.* **2003**, *32*, 406-407.

[34] Sattler, W.; Parkin, G. *Polyhedron* **2012**, *32*, 41-48.

[35] Kitajima, N.; Hikichi, S.; Tanaka, M.; Moro-oka, Y. *J. Am. Chem. Soc.* **1993**, *115*, 5496-5508.

[36] Liu, X.; Du, P.; Cao, R. *Nature Commun.* **2013**, *4*, 2375.